



# FRAG BLAST 11

## 11th International Symposium on Rock Fragmentation by Blasting

24–26 August 2015 | Sydney, Australia

### Proceedings

Proceedings Sponsor



Proudly hosted by



Supported by



# **11TH INTERNATIONAL SYMPOSIUM ON ROCK FRAGMENTATION BY BLASTING**

---

**24–26 AUGUST 2015  
SYDNEY, AUSTRALIA**

The Australasian Institute of Mining and Metallurgy  
Publication Series No 7/2014



**Edited by A T Spathis, D P Gribble, A C Torrance and T N Little**

Published by:  
The Australasian Institute of Mining and Metallurgy  
Ground Floor, 204 Lygon Street, Carlton Victoria 3053, Australia

# Dilution, Ore Grade and Blast Movement Calculation Model

J F D Domingo<sup>1</sup>, F S Leite<sup>2</sup>, V G Mirada<sup>3</sup> and I C Carrasco<sup>4</sup>

## ABSTRACT

This paper investigates ore loss and dilution produced by rock movement in bench blasting. A total of four blasts, in which electronic detonators have been used, were monitored in Cobre Las Cruces Open Pit Mine (FQM Ltd) in Gerena (Sevilla, Spain). Rock motion has been obtained in 137 points of the free face and 6 points inside the block. Multiple liner regression has been applied to predict rock motion and estimate ore dilution as a function of hole coordinates, rock contacts, powder factor/hole, amount of explosive per blasthole, burden, spacing, hole length, stemming length, explosive energy, hole row, subdrilling, blast sequence, stiffness ratio, blasthole distance to free face, rock density and Young's modulus. The model is statistically significant with a determination coefficient over 0.8. Rock motion measurements in 31 more points have been used to validate the model and to show a reduction in ore dilution.

## INTRODUCTION

The bench blasting method is used in most of open pit mines to allow removal of a predetermined rock mass volume. These mine deposits are highly heterogeneous with the ore disseminated in pockets of varying grade with an economic cut-off grade determined for the mine operation and as such, any material with less mineralisation is designated as waste. The ore is excavated and hauled to the mineral processing plant while the waste is transported to a suitable dumping location. Blasting of these rocks involves drilling a series of holes with a calculated spacing-burden ratio necessary to fragment and loosen the rock mass; however, the movement of the rock caused by blasting has an unfavourable effect on the ore and waste separation in the muck pile, causing either ore loss (the ore is wrongly categorised as waste and sent to the waste dump) and/or ore dilution (waste is wrongly categorised as ore and sent to the processing plant). The dilution or mineral loss has two important factors in the grade control of a mine. For example, in a blast zone with 7678 m<sup>3</sup> of mineral with a grade of 2.06 per cent, when diluted with 504.7 m<sup>3</sup> of waste at 0.81 per cent, decreases its initial grade by 24 per cent. This, for a long period of production, represents a reduction of the processing plant productivity and transportation of unwanted material; consequently, lower profits are achieved. The starting point of each dilution control study is to estimate the amount of material mixed during blast movement. This document presents a new formula for predicting the surface and internal motion as well as the dilution produced by it. This formula was deduced empirically from the study of 100 data from blasts and validated with 31.

## OBJECTIVE

The objective of the study is to develop a tool for estimating, controlling and minimising dilution in metal mining. For that, it was considered using electronic detonating technology and selective sequencing to decrease mineral mixture - decreasing the risk area in contact (Figure 1) - to facilitate the process of zoning and muck pile loading.

Essentially, in a blast, the dilution or loss of mineral are associated with:

- location of the blast (existence of contacts between different materials)
- blast design (hole position, charge distribution, stemming, etc)
- sequence and blast movement.

The two types of dilution that may occur are internal dilution (when this is produced by inclusion of waste existing inside an ore block) and dilution or external contact (when produced by the unfavourable movement of the boundary between two types of material, and some of the waste mixes with mineral). The external dilution is studied and estimated by monitoring blast parameters. Dilution (Ebrahimi, 2013) in a blast can be calculated from the percentage of waste (or material below a certain cut-off) that is mixed with the orebody during operation:

$$\% \text{ Dilution} = \frac{V_w}{V_T} \quad (1)$$

where:

$V_w$  is waste volume (m<sup>3</sup>)

$V_T$  is blast total volume (m<sup>3</sup>)

1. Mining Key Account Manager, MAXAM – Civil Explosives, Av Partenón 16, Madrid 28042, Spain. Email: jdomingo@maxam.net

2. Projects Engineer, MAXAM – Civil Explosives, Av Partenón 16, Madrid 28042, Spain. Email: fleite@maxam.net

3. Projects Engineer, MAXAM – Civil Explosives, Av Partenón 16, Madrid 28042, Spain. Email: vgouveia@maxam.net

4. Mine Planning Chief, First Quantum Minerals Ltd, Cobre Las Cruces SA, Ctra SE-3410 – Km 4,1, Gerena, Sevilla, Spain. Email: ivan.carrasco@fqml.com

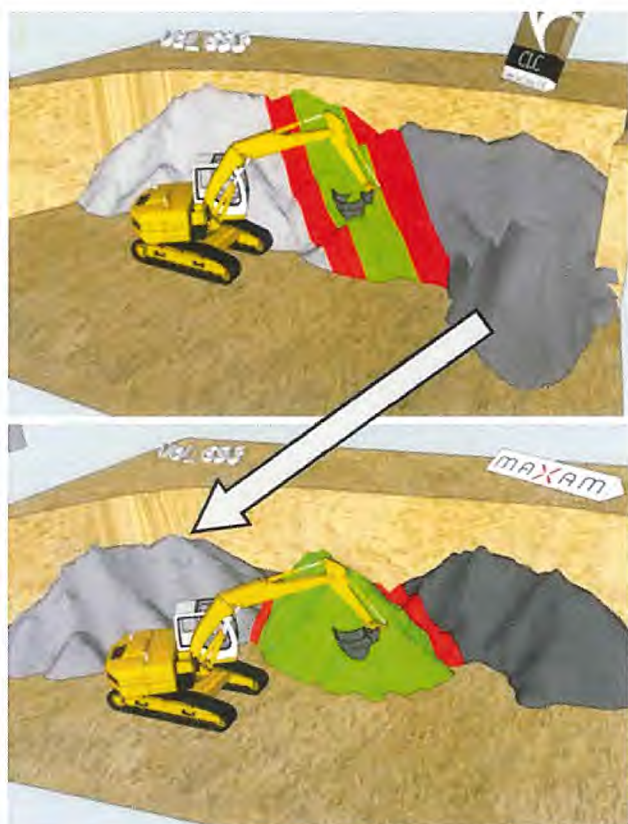


FIG 1 – Risk area.

The importance of dilution control or ore loss, mainly in metal mining, is associated with the construction of blending to standardise the grade of mineral entry into the treatment plant.

**PROBLEM IDENTIFICATION**

The grade control is based on examination and assessment of the drill cuttings of each hole and this delimits different zones types.

The theoretical blending construction is based in the initial grades of each blast zone so that the changes in grade

produced by the movement of the mass were not considered in the calculus. This situation can translate into a significance grade change in the point of entry in plant.

Table 1 compares the estimated blending without taking into account the movement of the blasted mass (theoretical) with those considering such movement (real). This part of the study used data from seven blasts and, as can be verified, the mixing during the blast process may provide a reduction of the final blending grade from about 3.50 per cent to 3.03 per cent or 4.20 per cent to 3.79 per cent. This phenomenon can be understood regarding the difference of the metallic Cu between forecasts and reality (\*), where the negative sign represents the tonnage not reaching its final destination.

To understand the importance of this situation, a series of blasting were analysed in economic terms:

- *Copper sent to waste (lost)* – for just three blasts (waste/mineral contact) mineral sent directly to waste was determined and 8.4 t of copper was estimated; this is equivalent to US\$50 984.78 (Table 2).
- *Copper transported to the wrong blending* – if diluted mineral is not moved to waste then it is transported to another blending and disturbs its theoretical grade. Indeed, we cannot refer to the concept of loss mineral; however, depending on the grade of the mixing material, the severity can be equal or greater than the loss of it. The estimated copper moved to a wrong destination reached the quantity of 565.25 t in seven blasts.

This situation could lead to a lower actual grade blending than predicted. When analysing the blending grade control on Figure 2 based on the blending study (Table 1), it is possible to affirm that actual blending grade was under the theoretical grade over the period of this study.

**Blasting study**

Database of the model is composed by measurements made in Cobre Las Cruces Mine (First Quantum Minerals, Ltd). General blasting scheme of Cobre Las Cruces can be seen in Figure 3. Blast parameters depending of the rock type are shown in Table 3.

TABLE 1  
Blending construction study.

Blending	Blast number	Theoretical			Real			Cu ton Difference (*)	% Cu control			
		Density	Volume	Ton	Density	Volume	Ton		% Cu theoretical	% Cu real	Difference	Error
A	4	3.84	5984.15	23254.19	3.83	5131.56	20079.52	-213.43	3.5%	3.03%	0.50%	-14%
C	1	3.85	3611.77	13908.77	3.87	3779.51	14642.97	24.45	2.7%	2.73%	0.03%	1%
D	4	3.61	5314.04	19312.50	3.61	4982.95	18071.40	-134.37	4.2%	3.79%	0.45%	-11%
E	5	3.94	4416.62	23709.02	3.90	4825.21	25067.90	8.26	5.9%	5.66%	0.29%	-5%
F	4	3.73	4786.09	18283.96	3.73	5321.06	20245.69	44.57	3.9%	3.73%	0.16%	-4%
G	4	3.88	7252.99	27903.49	3.85	8249.28	31631.08	145.35	6.6%	6.32%	0.32%	-5%
H	2	3.70	1567.75	5837.34	3.67	1562.03	5593.65	-11.23	2.9%	2.78%	0.08%	-3%
IEM	3	3.29	5969.16	5837.34	3.28	5048.46	17438.99	57.08	0.8%	0.58%	0.17%	-23%
SBL	4	3.45	7714.20	5837.34	3.45	6990.40	24313.37	261.77	1.6%	1.46%	0.14%	-9%
SM	2	3.70	2886.77	5837.34	3.71	3444.94	12929.15	125.49	2.0%	1.87%	0.12%	-6%
GA	2	2.82	1471.61	5837.34	2.82	1165.03	3383.18	-14.34	0.3%	0.12%	0.19%	-61%
SGE	1	2.98	474.57	5837.34	2.98	410.46	1221.72	-1.17	0.02%	0.00%	0.02%	-100%

**TABLE 2**  
Blast estimation mineral losses.

Blasts	3
Loss Cu (t)	8.4
\$/t (12/May/14 – InfoMine.com)	6939.0
Copper processing price/t	888.9
Loss (US\$) with production cost	50 984.78

**TABLE 3**  
Blast characteristics.

	Mineral	Waste
Density (kg/cm <sup>3</sup> )	3–4.2	1–4.12
Rock elasticity		
Drill diameter (mm)	140	152
Production holes B × S (m × m)	4 × 4	5 × 5
Cut holes B × S (m × m)	3 × 3.5	4.5 × 3
Bench high (m)	4.5–5	4.5–5
Free face angle (°)	90	90
Stemming (m)	2.5–3	2.5–3
Powder factor (kg/m <sup>3</sup> )	0.34–0.45	0.5–0.7
Delay between rows (ms)	150	150
Delay within rows (ms)	25	25
Explosive type	Heavy ANFO	Heavy ANFO
In-hole and surface initiation systems	Non-electric	Non-electric

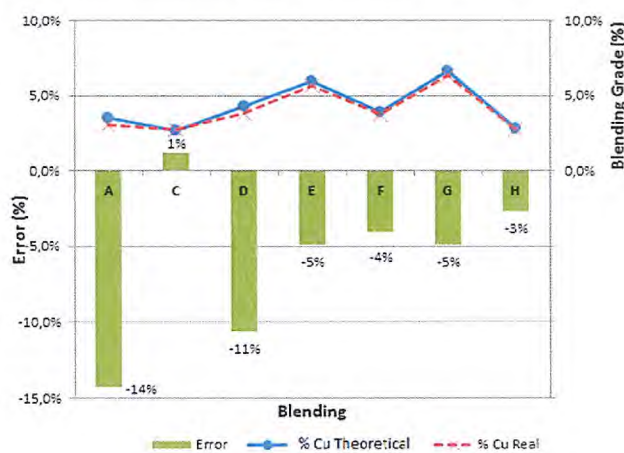


FIG 2 – Blending control grade.

**Key performance indicators**

A series of key performance indicators (KPIs) were selected (powder factor, charge per hole, burden, spacing, hole length, stemming, energy, row number, subdrilling, time between rows, time between holes in a row, stiffness ratio, distance to free face, rock density and rock elasticity) and each of them were compared with the surface and internal bench displacement.

**Surface movement**

The study of the surface movement was carried out by using a series of control units (ten per blast) introduced in the stemming (La Rosa and Thornton, 2011) of various determined holes. Their initial position (before the blast) and their final one (after the blast) were calculated and then movement blast maps were built (Figure 4). With the control unit movement vectors associated to the zone contact, it was possible to predict their movement. From the coordinates of the initial and final contact, it was possible to calculate the mixing area of each contact, and so, predict dilution, loss or gain (Taylor and Firth, 2003). A 3D laser (distances and horizontal angles were measured) was used to carry out the measurement of the points before and after a blast thereby generating its coordinates.

**Internal movement**

To understand the internal movement of a blast, the displacement (Thornton, Sprott and Brunton, 2005) of some blast zones were studied in six blasts. For this purpose, spring rubber and synthetic reinforced hoses with high tensile strength yarn in nitrile rubber coating were used. These materials were introduced into empty holes drilled between the production ones. In order to register the final shape of these control objects, GPS coordinates were taken with respect to depth.

The internal movement can be understood analysing the typical profile of a bench movement (Figure 5). It is possible to affirm that the bench movement displaces the rock in a convex/membrane curvature shape reaching its maximum point at half the bench high. For this reason, it was decided to use the mathematical equation of a membrane to represent the bench internal movement.

**Bench movement and membrane equation**

The function that defines the behaviour of a membrane is given by the wave equation:

$$M\Delta_u = \rho \frac{\partial^2 u}{\partial t^2} \tag{2}$$

where:

$M\Delta_u$  is dilation of membrane surface

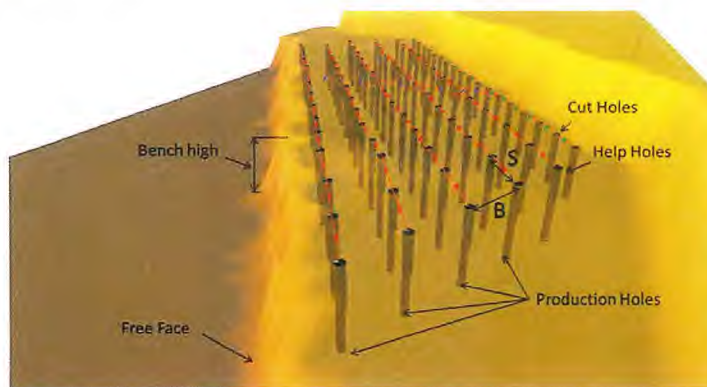


FIG 3 – Sketch of a typical blast.

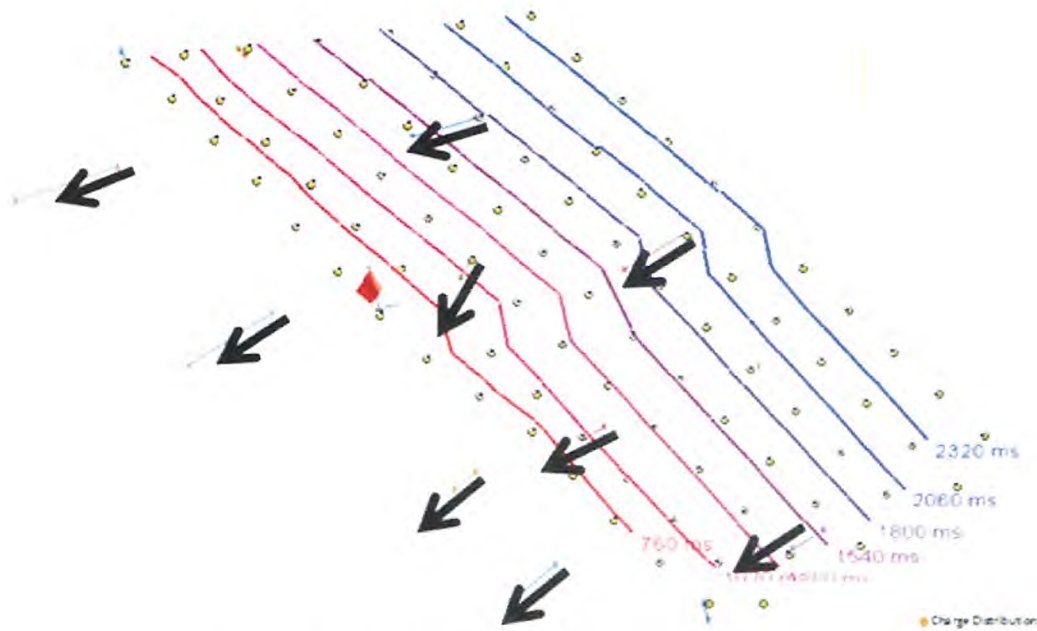


FIG 4 – Surface blast movement control (direction vectors and time iso-lines).

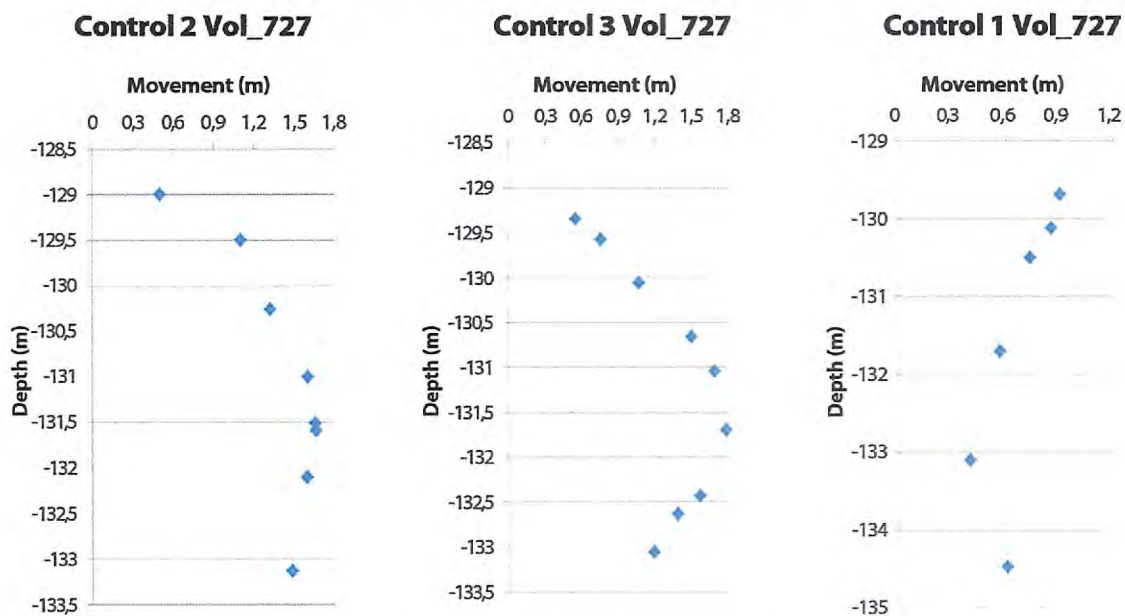


FIG 5 – Typical shapes of internal movement control.

$\rho$  is membrane density

Solving the equation we obtain:

$$M = K \sin\left(\frac{m\pi}{a}x\right) \sin\left(\frac{m\pi}{b}y\right) \cos\left((t - t^*) \sqrt{\frac{T\pi}{\rho} \left(\frac{n^2}{a^2} + \frac{m^2}{b^2}\right)}\right) \quad (3)$$

where:

$t^*$  is elapsed time of the membrane movement from its resting position to the maximum dilation

Nevertheless, in the maximum dilation point where  $t = t^*$ , then:

$$\cos\left((t - t^*) \sqrt{\frac{T\pi}{\rho} \left(\frac{n^2}{a^2} + \frac{m^2}{b^2}\right)}\right) = 1 \quad (4)$$

so that:

$$M = K \sin\left(\frac{x\pi}{a}\right) \sin\left(\frac{y\pi}{b}\right) \quad (5)$$

where:

$a$  is the horizontal dimension of the membrane

$b$  is the vertical dimension of the membrane

$x$  is the horizontal variation of the membrane

$y$  is the vertical variation of the membrane

Based on this equation, the bench movement phenomenon has been represented in Figure 6 so as to better understand it: I – perpendicular contacts to the typical bench movement; II and III – expansion of the membrane shape; IV – final contact deformed in the form of a membrane shape.

As it can be observed, the initial contacts are modified by the blast and the next step, as represented in Figure 7 is define the maximum displacement point (K).

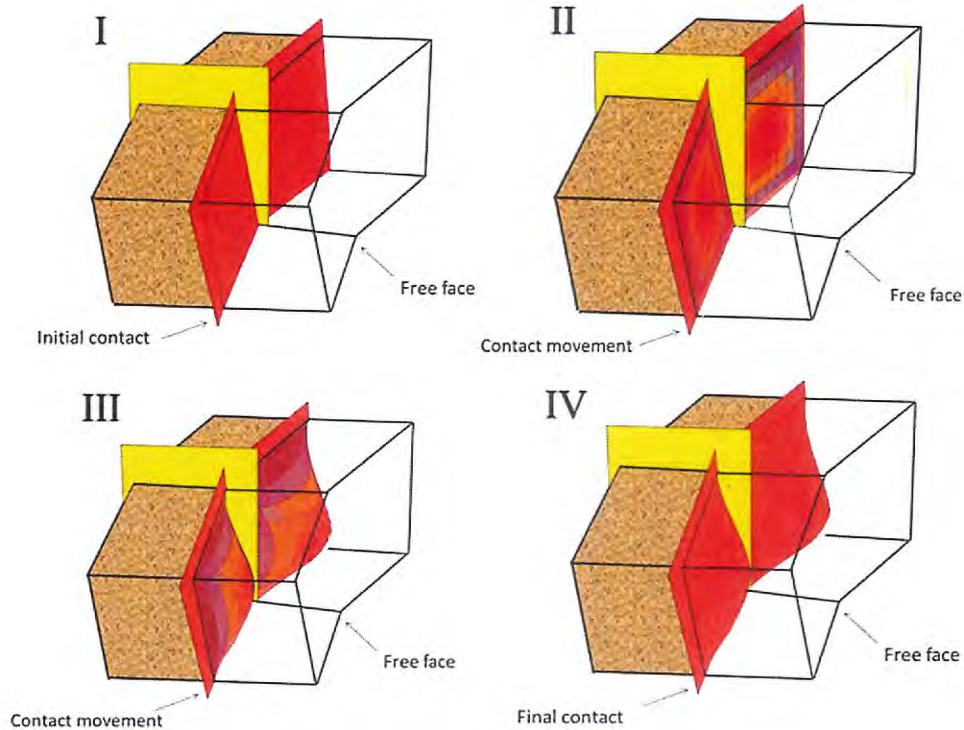


FIG 6 – Bench movement based on membrane equation.

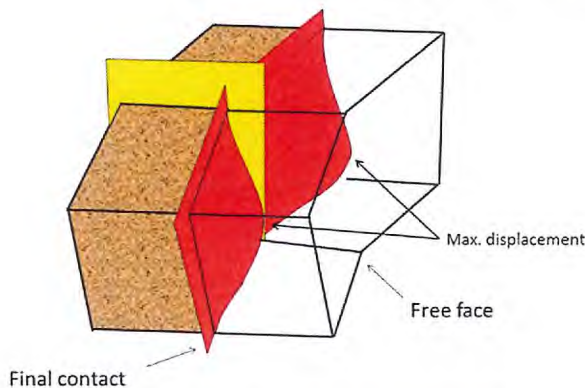


FIG 7 – Membrane's maximum displacement point.

**Model description**

The model description is separated in two phases:

1. data treatment – surface and internal movement
2. grade control and mixed volume estimation – dilution calculation.

For each set of data the multilinear regression method was used; variables with no significance were identified and dismissed. To confirm and characterise the regression as a model, residuals were analysed and proved (Kolmogorov-Smirnov and Shapiro-Wilk) that a normal distribution was followed (significance level more than 0.05).

**Surface movement**

From all the controls used in the study, 131 were selected to validate the model (100 for the formalisation and 31 for the validation). The surface movement equation obtained with a coefficient of determination of 80.3 per cent with a significance level of 0.069 (Kolmogorov-Smirnov) and 0.128 (Shapiro-Wilk) was:

$$D = \frac{0,089}{\log(PF)} + 0,121 \times B^2 - 0,944 \times \log(S) + 0,256 \times R^2 - \frac{0,006}{\log(SB)} - \frac{0,031}{V^2} - \frac{1,579}{(SR)^2} + \frac{3,117}{Row^2} \tag{6}$$

where:

- D is the surface displacement (m)
- PF is the powder factor (kg/m<sup>3</sup>) =  $\frac{Q}{B \times S \times L}$
- Q is the explosive charge (kg)
- L is the hole length (m)
- B is the burden (m)
- S is the spacing (m)
- V is the blast velocity (m/s) = (S/T)
- T is the delay
- R is the stemming length (m)
- SB is the subdrilling (m)
- SR is the stiffness ratio (HB/B)
- HB is the bench high (m)
- row is the row number

**Internal movement**

For the membrane dilation calculation the parameter that define it maximum value is K.

Using the same methodology with a coefficient of determination representing 97.6 per cent of the data, with a significance level of 1.79 (Kolmogorov-Smirnov) the maximum dilation of the membrane was obtained as follows:

$$K = -0,304 \times \rho_{rock} + 5,038 \times PF - 0,008 \times \Delta_{FF} \tag{7}$$

where:

- K is the maximum dilation of the membrane (m)
- PF is the powder factor (kg/m<sup>3</sup>) =  $\frac{Q}{B \times S \times L}$
- $\rho_{rock}$  is the rock density (g/cm<sup>3</sup>)
- $\Delta_{FF}$  is the distance to free face (m)

Taking into account the described  $K$ , the membrane volume can be obtained by the integration of:

$$V_M = \int_0^a \int_0^b M \, dy \, dx \quad (8)$$

$$V_M = \frac{4ab}{\pi^2} \times K \quad (9)$$

### Dilution and final grade calculation

As dilution is directly associated with the mixed volume, it is important firstly to define that volume. A determined volume of a blasted zone is characterised by the surface movement and the inputs and outputs caused for the internal movement of this zone (Figure 8).

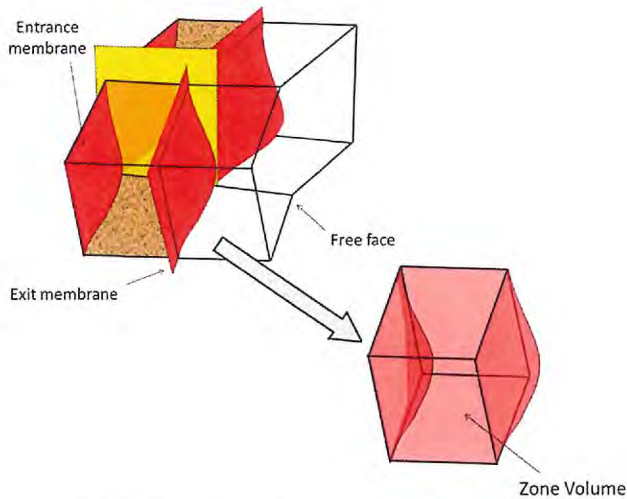


FIG 8 – Entrance and exit membrane and final zone volume.

The volume of the mixed zone defined by the surface movement is:

$$V_{TS} = A_f \times H \quad (10)$$

where:

$V_{TS}$  is the volume of the mixed zone considering surface movement ( $m^3$ )

$A_f$  is the area defined by the final position of contacts ( $m^2$ )

$H$  is the bench height (m)

However, the volume of the mixed zone, considering the internal movement, is described by:

$$V_T = A_f \times H + V_{MI} - V_{MO} \quad (11)$$

where:

$V_T$  is the volume of the mixed contact considering the surface and internal movement ( $m^3$ )

$V_{MI}$  is the input membrane volume ( $m^3$ )

$V_{MO}$  is the output membrane volume ( $m^3$ ) (see Figure 8)

Once volumes representing ore or waste have been defined, the dilution or loss can be calculated.

When  $V_{MI}$  refers to waste,  $V_{MIW} = V_{MI}$  and when  $V_{MO}$  refers to ore,  $V_{MOO} = V_{MO}$ , then dilution and loss can be defined by:

$$\text{Dilution}(\%) = \frac{V_{MIW}}{V_T} \quad (12)$$

$$\text{Loss}(\%) = \frac{V_{MOO}}{V_T} \quad (13)$$

where:

$V_T$  is the volume of the mixed contact considering the surface and internal movement ( $m^3$ )

$V_{MIW}$  is the input waste volume ( $m^3$ )

$V_{MOO}$  is the output ore volume ( $m^3$ )

The final grade zone calculation (Wang *et al*, 2011) is based on a mass balance between zones. In this way, the final percentage of each element can be calculated with the formula below:

$$G_F = \frac{(G_0 \times V_0 \times \rho_0) + (G_{MI} \times V_{MI} \times \rho_{MI}) - (G_0 \times V_{MO} \times \rho_0)}{V_0 \times \rho_0 + V_{MI} \times \rho_{MI} - V_{MO} \times \rho_0} \quad (14)$$

where:

$G_F$  is the final zone grade (per cent)

$G_0$  is the initial zone grade (per cent)

$V_0$  is the initial zone volume ( $m^3$ )

$\rho_0$  is the initial zone density ( $g/cm^3$ )

$G_{MI}$  is the input contact grade (per cent)

$\rho_{MI}$  is the input contact density ( $g/cm^3$ )

### DELAY SEQUENCING RESULTS AND DISCUSSION

In addition to the dilution control model developed, different types of sequencing were compared for a given blast with the aim of testing the best design to prevent dilution.

So, two zones (low grade and medium grade) were analysed. First a non-electric sequencing system was used; data have been introduced in the above created model taking into account surface and internal displacements. Sequencing and results can be observed in Figure 9.

According to grade control a decrease in grade in three of the four zones divided by the contact areas was obtained: -9.60 per cent (Z2), -3.85 per cent (Z3) y -1.01 per cent (Z4) respectively. The grade in Zone 1 was increased (as expected) since material in Zone 2 (higher grade) had mixed with the former. As already discussed, these differences on a large scale can jeopardise the blend construction. There was 13.6 per cent dilution in this blast.

Another blast in the same area as previous analysed blast was made using electronic detonators and employing selective sequencing (Figure 10).

With this type of sequence and introducing data in the model, superficial and internal blast movement are represented. It was found that the decrease of grade was -0.044 per cent (Z2), -0.06(Z3) y -0.4(Z4). As expected, Zone 1 had a slight rise in grade of only 0.105 per cent. With respect to dilution, a value of 5.7 per cent was obtained – a value extremely low as compared to the value registered for non-electric detonators.

This data reflects a clear optimisation in the grade control through blast design using electronic detonators in such a way that its use is advocated for these situations.

The visual result has been clearly satisfactory in employing this methodology. As observed in Figure 11, there was the formation of three muck pile mounts from the detonation of the central holes of each zone and its consequent valleys in the borders of the zone.

After marking contacts topographically, as seen in Figure 11, it can be verified that they are located in the valleys generated by the sequence design employed.





FIG 9 – Displacement model – non-electric initiation.



FIG 10 – Displacement model – electronic initiation.

**CONCLUSIONS**

To develop a prediction model for dilution, measurement techniques for surface and internal blast movement were established. Such techniques showed an extremely useful application for the mentioned model. The model has been validated, being that it passed all the normality tests that it was subjected to. This confirmed the uncertainty of the blend construction based on materials separated in blasts designed with non-electric detonators (up to a 14 per cent difference of the proposed grade) and achieved ascertaining the improvements in blend construction with electronic detonator initiation system.

A loss of about US\$60 000 was estimated in only three blasts. These values are significant when extrapolated to the end of a year of work, hence clearly justifying that

investment in such studies can cause a reduction of more than 50 per cent of the estimated loss. This reduction is based on the difference in the volume of mineral lost in a blast using a non-electric initiation system and an electronic initiation system with values of 1234.37 m<sup>3</sup> and 545.93 m<sup>3</sup> respectively.

To carry out these studies, the definition of each blasting area before designing a sequence is of great importance and this requirement has been achieved by Cobre Las Cruces.

The use of electronic detonators corroborated an expected reduction in dilution from 14 per cent to 5.7 per cent. The design of a selective sequence involves a more detailed study of the blast. Nevertheless, the obtained results from the study were highly satisfactory.

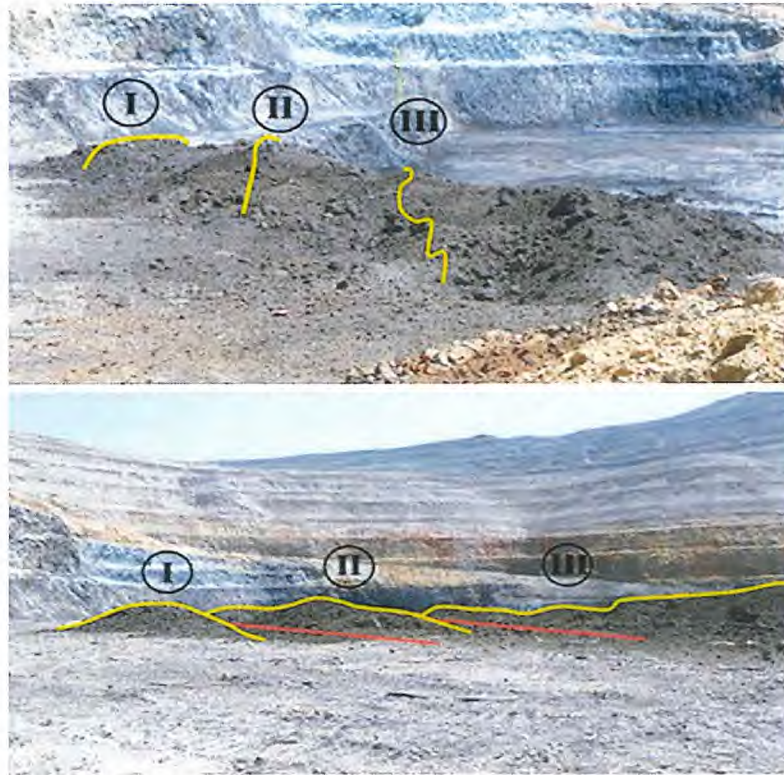


FIG 11 – Peak valleys from electronic initiation.

A decrease in the dilution enables the construction of a more reliable blending and an optimised exploitation of the grade present in the deposit under study.

In terms of blast design for short and long time detonations within contacts, it was concluded that the former allows a better separation between zones, hence the borders of this being formed by valleys produced by the movement of the rock.

The separation of zones of equal grade for the construction of two distinct blending is of equal importance as the others. Avoiding the mixture between zones and the danger of grade reduction curtail the risk of uncertainties in the blending control data.

**ACKNOWLEDGEMENTS**

First Quantum Minerals, especially for their trust, support and opportunity to carry out the field work in Cobre Las Cruces Mine (FQM, Ltd). To Javier Cañal (First Quantum Minerals Ltd, Cobre Las Cruces), Bartolomeo Borreguero (GPV) and to all the blast and load and haul personnel (GPV-AOMSA-EPSA) who were involved during the field data collection are acknowledged for their patience and help. To Rosa Cazallas for the essential support in the development of the model application tool. We would like to thank the geology,

grade control, topography personnel (Cobre Las Cruces) and Cristina Pardo (CLC-intern) for the support during the KPI gathering process.

**REFERENCES**

Ebrahimi, A, 2013. An attempt to standardize the estimation of dilution factor for open pit mining projects, presented to 23rd World Mining Congress, August, Montreal.

La Rosa, D and Thornton, D, 2011. Blast movement modelling and measurement in *Proceedings 35th APCOM Symposium 2011*, pp 297-310 (The Australasian Institute of Mining and Metallurgy: Melbourne).

Taylor, D L and Firth, I R, 2003. Utilization of blast movement measurements in grade control, in *Proceedings Application of Computers and Operations Research in the Mineral Industries*, Reno, pp 243-248 (South African Institute of Mining and Metallurgy: Marshalltown).

Thornton, D, Sprott, D and Brunton, I 2005. Measuring blast movement to reduce ore loss and dilution, in *Proceedings 31st Annual Conference on Explosives and Blasting Technique 2005*, pp 189-200 (International Society of Explosives Engineers: Cleveland).

Wang, W, Huang, S, Wu, X and Ma, Q, 2011. Calculation and management for mining loss and dilution under 3D visualization technical condition, *Journal of Software Engineering and Applications*, 5(5):329-334.

# AUTHOR INDEX

<b>A</b>			
Abedi, A	161	Drebenstedt, C	755
Abeel, P	211	Duan, Y	593
Adamson, W R	3	Duggan, R	189
Adermann, D	471	<b>E</b>	
Adiyansyah, B	307	Ebrahimi Farsangi, M A	315, 685
Aimone-Martin, C	211	Esen, S	189, 409
Araos, M	565	Esmaeili, K	377
Avilés, D	625	<b>F</b>	
Aziznejad, S	377	Faramarzi, F	315, 685
<b>B</b>		Ferrari, A J D	363
Balachander, R	801	Finoti, L	749
Battison, R	189	Fonseca, A L S	363
Bettencourt, J	267, 355, 749	Fourney, W L	27
Beyglou, A	385	<b>G</b>	
Bhandari, A	393	Gabriel, E	401
Bhandari, S	393, 455	Galvão, F	355, 749
Blair, D P	13, 203	Gao, Q D	79
Blay, K R	297	Garg, R	393
Brent, G	635	Gaunt, J	307
Brown, P	429	Genge, D	645
<b>C</b>		Golin, F	267
Cardu, M	267, 355, 749	Gomes, A	401
Caron, K	333	Gopinath, G	801
Carrasco, I C	71	Gorinov, S A	555
Castedo, R	57, 545, 819	Goswami, T	635, 645
Cavanough, G	477	Green, A	429
Chalmers, D	471	Green, B	599
Chen, M	79, 673	Gupta, N	455
Chen, Z-Y	169	<b>H</b>	
Chiquito, M	819	Hakami, A	315
Cho, S-H	809	Hamdi, E	89
Crispin, P	401	Hassell, R	221
Cunha, E B	363	Hawke, S J	321
<b>D</b>		Henley, K	189, 485
Dare-Bryan, P	189, 429	Hosseinzadeh Barforoosh, A	161
Deb, D	65	Hu, Y G	79
Dehghan, M R	315	<b>I</b>	
del Castillo, I	545	Ibarra, R	575
De Tomi, G	355, 749	Ivanova, R	693
de Vries, R	221	<b>J</b>	
Diaz, R	333	Jahani, M	707
Domingo, J F D	71	Jaitawat, P S	533
Dominguez, L A	321		
Dowding, C	211		

Johansson, D	<b>385, 493, 585, 793</b>	Munaretti, E	<b>267</b>
Johansson, N	<b>385</b>	Muñoz, C	<b>625</b>
Joshi, A	<b>279, 437, 533</b>	Murthy, V M S R	<b>501</b>
Julian, L	<b>511</b>	Musunuri, A	<b>511</b>
<b>K</b>		<b>N</b>	
Kanchibotla, S S	<b>307, 511</b>	Nagarajan, M	<b>409, 429</b>
Karrech, A	<b>89</b>	Navarro, J	<b>819</b>
Katsabanis, P D	<b>715</b>	Nordqvist, A	<b>493, 763, 775</b>
Kennelly, L	<b>307</b>	Norgard, J	<b>579</b>
Kharitonenko, I	<b>417</b>	Noy, M J	<b>721</b>
Kim, H-S	<b>809</b>	Nyberg, U	<b>585, 727</b>
Kim, J-K	<b>809</b>	<b>O</b>	
Kim, S-J	<b>809</b>	Olsson, A	<b>477</b>
Klaric, P	<b>327</b>	Olsson, M	<b>727</b>
Koppe, J C	<b>267, 289, 401</b>	Omidi, O	<b>715</b>
Ko, Y-H	<b>809</b>	Onederra, I	<b>149, 565</b>
<b>L</b>		Oosthuizen, T	<b>425</b>
Laing, T J	<b>527</b>	Ortega, N	<b>625</b>
La Rosa, D	<b>333</b>	Osterman, R	<b>233</b>
Lawlor-O'Neill, M L	<b>97</b>	Ouchterlony, F	<b>109, 257, 693, 727</b>
Leite, F S	<b>71</b>	<b>P</b>	
Leslie, K E	<b>297</b>	Pablos, I	<b>401</b>
Li, L F	<b>463</b>	Papillon, B E	<b>417, 575</b>
Little, T N	<b>343</b>	Parihar, C	<b>393</b>
Liu, W Z	<b>463, 815</b>	Park, H	<b>809</b>
López, L M	<b>57, 545, 819</b>	Parra, H	<b>121</b>
Lu, W B	<b>79, 673</b>	Paswan, R K	<b>279</b>
<b>M</b>		Petropoulos, N	<b>493, 775</b>
Mamani, H	<b>333</b>	Player, J	<b>221</b>
Mansouri, H	<b>315, 685</b>	Popov, P	<b>417</b>
Marin, T	<b>355</b>	Pramanik, R	<b>65</b>
Martin, C	<b>471</b>	Prasad, B	<b>755</b>
Martin, D	<b>519</b>	Preece, D S	<b>127, 617</b>
Martin, E	<b>645</b>	Preston, C	<b>137</b>
Martins, P A A	<b>363</b>	<b>R</b>	
Maslov, I Y	<b>555</b>	Raina, A K	<b>501</b>
Matthew, V O	<b>363</b>	Rajmeny, P	<b>437</b>
McKenzie, C K	<b>417</b>	Ren, G	<b>169</b>
McNamara, G	<b>307</b>	Rezende, A	<b>355, 749</b>
Melo, E	<b>355</b>	Richards, A B	<b>527</b>
Mihaylov, D	<b>493</b>	Rigby, G	<b>579</b>
Minchinton, A	<b>41</b>	Righetti, E	<b>775</b>
Mirada, V G	<b>71</b>	Rock, J	<b>477</b>
Mitri, H S	<b>245</b>	Romero Huerta, J	<b>749</b>
Mohanty, B	<b>607</b>	Rothery, M	<b>645</b>
Moore, A J	<b>527</b>	Roy, D	<b>137</b>
Moser, P	<b>257, 693</b>	Roy, M P	<b>279, 533, 755</b>
Muller, K	<b>425</b>		

**S**

Sadao, G	749
Sainoki, A	245
Sanchidrián, J A	57, 545, 741, 819
Santos, A P	57, 819
Sarim, M D	533
Schaarsdmit, R	401
Schimek, P	257
Schunnesson, H	385
Scott, A	149, 447
Seccatore, J	267, 355, 749
Segarra, P	57, 545, 819
Sellers, E J	307, 511
Shekhawat, L S	279, 437
Shi, Q Q	815
Shrimali, R	437
Silling, S A	127
Silva, A C	363
Silva, E M S	363
Silva, V M	363
Singh, P K	279, 533, 755
Singh, S P	369
Singh, T N	455
Solis, H	575
Spathis, A T	97, 297
Svedensten, P	727
Symonds, D	307

**T**

Taji, M	161, 707
Tawadrous, A	127, 617
Teowee, G	575
Thomson, S	579
Thurley, M J	763, 775
Torrance, A C	447, 477
Trivedi, R	455

**U**

Uttarwar, M D	655
---------------	-----

**V**

Valery, W	333
Van Doorselaere, D	369
Venkatesh, H S	801
Vergara, J	625
Vieira, L	289
Vilela, D R T	363
Villaescusa, E	221

**W**

Wang, F	593
Wang, G H	673
Wang, Y M	463
Wellink, S	471
Wheeler, B	127
Widenberg, K	727
Wilkinson, D	579
Williams, T	137
Wimmer, M	493, 763, 775

**X**

Xiong, D	593
Xu, G	593

**Y**

Yang, H-S	809
Yang, H T	815
Yang, J	169
Yang, R	177
Yan, P	79, 673
Yao, L	593
Yerpude, R R	655
Yi, C	585, 793
Yu, Q	169

**Z**

Zenteno, D	121
Zhang, Q B	665
Zhang, X L	463, 815
Zhao, J	665
Zhou, J R	673
Zwaan, D	607